Reconstruction

July 4, 2018

Contents

1 Reconstruction

While in the past Cherenkov detectors have been very successful in reconstructing various properties of the particles involved in a neutrino event, liquid scintillation detectors have long been thought as a source for calorimetric information only. However, in recent years it became obvious that the time information of the light in liquid scintillators can be used to access a wide range of information, similar or even superior to what a pure Cherenkov detector can deliver.

Basically, there are two complementary approaches to reconstruction in both detector types and consequently also in WBLS detectors. The first approach developed in MiniBooNE [] and successfully applied in T2K [] follows a likelihood ansatz to find the optimal track parameters and compare different hypotheses. In contrast to this, the three-dimensional topological reconstruction tries to picture the spatial distribution of the energy deposition within the detector without using a specific hypothesis. This technique has been developed for the LENA [] detector and successfully been used for muon events in Borexino. These are liquid scintillator detectors, but the application to Cherenkov detectors is straight forward.

Both methods have been improved considerably over the last couple of years. For example fitQun, the reconstruction software used by T2K is now able to reconstruct up to 6 Cherenkov rings. This alone will increase the expected sensitivity for example for CP-violation in the LBNF beam significantly in comparison to previous studies like []. In addition, the topological reconstruction promises large volume liquid detectors the same capabilities as only highly segmented detectors used to have (with all the implications of that). This includes possibilities for particle identification at energies as low as a few MeV based on topological information. This ability will be further enhanced by the combination of the two light species, Cherenkov and scintillation light, as can be seen in [Andrey], where Cherenkov-Scintillation separation is used to identify the two electrons of a $0\nu\beta\beta$-decay.

To give an overview on the state of the art in reconstruction, this section is divided into four subsections. The first subsection is dedicated to the likelihood approach and its latest results. The second subsection describes the topological reconstruction and its application to high energy events at the GeV scale and low energy events at the MeV scale. The third subsection is dedicated to applications of Cherenkov-light-Separation at low energies. Finally, we comment on other approaches like .....

1.1 Likelyhood

This subsection summarizes the main features of the reconstruction method developed for the MiniBooNE detector[**?**]. In this method a likelihood function is evaluated for a particle (particles) of some type with initial kintmatic parameters to have produced the observed collection of PMT hits, charges and times, in an event. A key ingredient of the likelihood calculation is the predicted hit distribution which represents the average response of the detector for such a particle and therefore the likelihood is a function of the paricle's kinematic parameters. The optimal parameters would provide the best agreement between the predicted and observed hit distributions i.e. the likelihood function will be at a maximum.

Realistic model of detector response is required to develop a successful and efficient event reconstruction and identification algorithms. This requires both *in-situ*

and *ex-situ* measurements of various optical properties of the water, PMTs and the reflection of all surface inside the detector. Absorption, scattering, reflections and fluorescence processes can affect the reconstruction. In order to account for these effects in the reconstruction, these optical properties have to be obtained if unknown.

Single track is parametrized with 7 parameters: starting point (x_0, y_0, z_0), starting time t_0, direction θ_0, ϕ_0 with respect to the beam and kinetic energy E_0. We refer to this vector as $\mathbf{u}$. Track information is obtained by maximizing the likelihood that track with vector $\mathbf{u}$ will produce the observed PMT measurements. The likelihood for an event assuming all PMTs are independent is given by

$$L(\mathbf{q}, \mathbf{t}; \mathbf{u}) = \prod_{i}^{N_{unhit}} P_i(\text{unhit}; \mathbf{u}) \times \prod_{j}^{N_{hit}} P_j(\text{hit}; \mathbf{u}) f_q(q_j; \mathbf{u}) f_t(t_j; \mathbf{u}). \tag{1}$$

Here $P_i(\text{unhit}; \mathbf{u})$ is the probability PMT i is not hit given $\mathbf{u}$, $P_i(\text{hit}; \mathbf{u})$ is the probability PMT i is hit given $\mathbf{u}$, $f_q(q_j; \mathbf{u})$ is the probability density function for the measured charge q given $\mathbf{u}$ and predicted charge q_j, $f_t(t_j; \mathbf{u})$ is the probability density function for the measured time t given $\mathbf{u}$ evaluated time t_j. Product is carried over all PMTs. For convenience we can work with the negative logarithm of the likelihood which can be written as a sum of negative logarithms. We will use F_q and F_t to denote the charge and the time negative logarithm likelihoods respectively

$$-\log L(\mathbf{u}) \equiv F_q(\mathbf{u}) + F_t(\mathbf{u}), \tag{2}$$

$$F_t(\mathbf{u}) = -\sum_{i}^{N_{hit}} \log f_t(t_i; \mathbf{u}), \tag{3}$$

$$F_q(\mathbf{u}) = -\sum_{i}^{N_{unhit}} \log P_i(\text{unhit}; \mathbf{u}) - \sum_{i}^{N_{hit}} \log P_i(\text{hit}; \mathbf{u}) - \sum_{i}^{N_{hit}} \log f_q(q_i; \mathbf{u}). \tag{4}$$

From here on we will refer to F_q and F_t simply as the charge and the time likelihoods.

If the number of observed photoelectrons (PE), n_i, is known for a given PMT one can assume that $f_q(q_i; \mathbf{u})$ is fully specified regardless of detector properties. In addition, n_i can be assumed to be Poisson distributed with a mean value $\mu_i(\mathbf{u})$ (predicted charge) for which the notation μ_i will be used with implicit dependence on $\mathbf{u}$. As a result, the probability for a PMT to have no hit is

$$P_i(\text{unhit}; \mathbf{u}) \equiv \overline{P}_i(\mu_i) = e^{-\mu_i}. \tag{5}$$

Hence, the probability a PMT has recorded a hit is

$$P_i(\text{hit}; \mathbf{u}) \equiv P_i(\mu_i) = 1 - \overline{P}_i(\mu_i). \tag{6}$$

The next step is to separate the predicted charge into prompt and late predicted charge

$$\mu_i \equiv \mu_{prompt,i} + \mu_{late,i}. \tag{7}$$

The prompt predicted charge is a result of Čerenkov light, while the late predicted charge has contributions from direct Čerenkov light and indirect light. Sources of indirect light are reflections, scattering and fluorescence.

Time PDFs $f_t(t_i; \mathbf{u})$ depend on the first photon to fire the PMT. Dependence on $\mathbf{u}$ can be reduced by introducing corrected time

$$t_{cor,i} = t_i - t_0 - \frac{r_{mid,i}(E_0)}{c_n} - \frac{\Delta s_{mid}(E_0)}{c}, \tag{8}$$

where t_i is the measured PMT time, t_0 is the measured start time, $\Delta s_{mid}(E_0)$ is the distance from the track start point to the mean Čerenkov emission point, $r_{mid,i}(E_0)$ is the distance from the mean Čerenkov emission point to the PMT, c_n and c are the speeds of light in water and vacuum respectively. Due to the latency period PMT can register only one hit for a given track. Probabilities of no prompt PEs and no late PEs can be written as $P(\text{no prompt PEs}) = e^{-\mu_{prompt}}$ and $P(\text{no late PEs}) = e^{-\mu_{late}}$ respectively. The probability that a hit contains at least one prompt PE is

$$w_p = P(\text{prompt PE present}|hit) = \frac{1 - P(\text{no prompt PEs})}{1 - P(\text{no prompt PEs})P(\text{no late PEs})}. \tag{9}$$

This is the weight for the prompt primitive distribution $G_{ch}(t_c, E_0, \mu_{prompt})$, while the $w_l = 1 - w_p$ is the weight for the late primitive distribution $G_{late}(t_c, E_0, \mu_{late})$. Finally, the time PDF is obtained from

$$f_t(t; E_0, \mu_{prompt}, \mu_{late}) = w_p G_{ch}(t_c, E_0, \mu_{prompt}) + w_l G_{late}(t_c, E_0, \mu_{late}). \tag{10}$$

The primitives distribution are created by generating particles throughout the detector in special runs (e.g. only Čerenkov light and no scattering) and the response is parametrized.

1.2 3D topological reconstruction

In this subsection a reconstruction method is presented which aims to provide a 3D topological representation of the energy deposition of an event. As the topology in question can have an arbitrary form, a method is needed which is not based on a hypothesis concerning the event type or rather the geometrical appearance of the energy deposition. Therefore, the only assumptions made within this method are that a reference point on the topology is known reasonably well in space and time (the time of the energy deposition) and that all particles propagate through this point in approximately straight lines with the speed of light. The necessary reference point has to be provided by a prior analysis of the event. In order to get information not only on likely points of energy deposition but also on the amount of energy deposit at each point, the full timing information of an event has to be used. This is in contrast to the other two methods in this paper where only the time of the first hit of each PMT is exploited. In the case that only the first hit time is known, this method can - after some adaptations - still be useful to provide pure topological information but the amount of energy deposition at each point is not easily reconstructable.

Basic idea

The general idea here is to use the timing information of all registered signals for the construction of isochronal surfaces around each light sensor defined by the signal time. The overlap of these surfaces then indicates likely points of origin of the

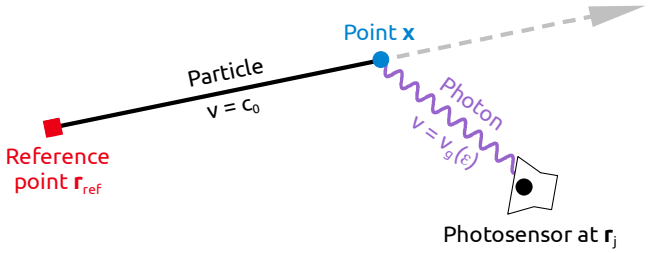

Figure 1: Illustration of the basic part of the information transport model used in the topological reconstruction. Passing the reference point r_{ref} at the reference time t_{ref}, a charged particle travels with the speed of light in vacuum c_0 along a straight track through x. A photon thereby emitted with energy ϵ at point x reaches the photosensor at r_j with the speed equal to the energy-dependent group velocity $v_g(\epsilon)$.

detected photons and thus can reflect the spatial distribution of the energy deposition of an event. For a point-like photon emission source each signal time corresponds to a spherical surface around the light sensor (PMT)[1]. By overlapping spheres around different PMTs the point source can then be located. For extended events this approach has to be modified, because it is not clear from which point of the event topology a given detected photon originated. Thus the time of flight of the particle acts as an offset to the signal arrival time. Therefore, the ansatz of simply using spheres with a radius corresponding to the time of the signal is limited. However, with some very simple approximations similar surfaces can be generated for extended events.

We only have to assume that all particles involved in an event propagate with the speed of light c directly away from the primary vertex. The total time t_{signal} between the start of the event and the arrival time of a scintillation photon at a given PMT can then be separated into two parts: The time it takes for the particle to propagate from the vertex V to the emission point X of the scintillation photon and the time the scintillation light needs from this emission point to reach the PMT P. This leads to the equation

$$c \cdot t_{signal} = |\overline{VX}| + n \cdot |\overline{XP}| \ , \tag{11}$$

where n is the effective refraction index for the scintillation light, $|\overline{VX}|$ is the distance between the vertex V of the event and the point of photon emission X, while $|\overline{XP}|$ is the distance between the point X and the PMT P (see Fig. 1). This formula describes surfaces which have a drop-like shape as seen in Fig. 2. This implies that – given a prior knowledge of the vertex and the time of the interaction at this point – drop-like surfaces can be constructed around each PMT P which contain all the possible points of origin X for a signal arriving at a time t_{signal}. Overlapping these drop-like surfaces of all signals involved will then give an impression of all points where photons have been generated, i.e. the event topology.

Several important aspects have to be noted at this point. First, it is essential to have a reference point on the event topology. The natural choice for this reference

[1]Since PMTs are still the most common light sensors used in large volume liquid detectors, we will refere to the light sensors as PMTs in the following text. However, in principle every kind of light sensor is suited as long as it can detect single photons.

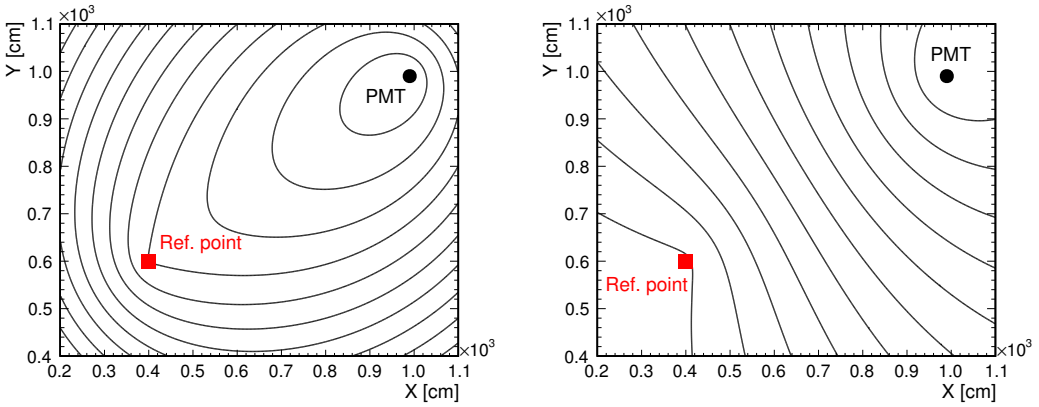

Figure 2: Isochrones in 2D for different values of $\hat{t}_j(x)$ from eq:RecoTimeModel with the plus (left) or minus (right) sign for the term describing the particle contribution. In the computation of $\hat{t}_j(x)$ relative to the reference point (red square) at $(400, 600)$cm, t_s was set to zero and $t_{\mathrm{ph}}(x, r_j)$ was calculated as the time of flight for a direct path from x to the photosensor (black circle) located at $(990, 990)$cm. For simplicity, the phase velocity $v = c_0/n$ with the refractive index $n = 1.484$ was used for the photon.

point is the primary vertex, but any point on the topology is suitable. However, if the reference point is not the primary vertex, a second set of surfaces is necessary instead of only using the drop-like shapes. This second type of surfaces occurs if you allow parts of the topology to lie backward in time with respect to the reference point. Then, Equation 11 has to be modified with a minus sign in front of the propagation part $|\overline{VX}|$ and thus every signal produces a second hyperbola-like surface which also contributes to the set of allowed points of origin for every detected photon. For the sake of simplicity, we will always assume in the following that we know the primary vertex with sufficient accuracy.

The next important aspect that has to be considered is the quality of the time signal. In reality, the signal time will not correspond perfectly to the sum of particle and photon propagation time, but rather will follow a certain time distribution. Thus, in general the emission point will not lie exactly on the drop-like surface. To take this into account, the drop-like shape has to be smeared with the time distribution of the signals expected from the detector properties. In other words, the infinitesimally thin surface aquires a profile. The shape of this profile perpendicular to the surface is given by the expected time distribution. A suitable time distribution for scintillation light is a convolution of a Gaussian, representing the time resolution of the photo detectors, and an exponential function, representing the emission time of scintillation photons due to de-excitation with different time constants:

$$F(t) = \sum_i a_i \cdot \frac{\lambda_i}{2} \cdot e^{-\lambda_i((t-t_{signal})-\frac{\lambda_i\sigma^2}{2})} \cdot \left[1 + erf(\frac{(t-t_{signal})-\lambda_i\sigma^2}{\sqrt{2}\sigma})\right] \qquad (12)$$

Here $\lambda_i = 1/\tau_i$ is the i-th decay constant of the scintillator and a_i is the fraction of the corresponding decay component with $\sum_i a_i = 1$. In total, we get a probability

density distribution describing the probability of a signal photon to be emitted from a given point X, which can be written as

$$P(\vec{x}) = F(t(\vec{x})) = F\left((|\overline{VX}| + n \cdot |\overline{XP}|)/c\right) \ . \tag{13}$$

However, this formula is still incomplete since the probability of a photon to originate from certain parts of the drop-like shape also depends on their position with respect to the PMT. Effects to be considered are: The signal attenuation in the liquid scintillator, the effective PMT area depending on the distance and the angle of a given point with respect to the PMT, and an angular acceptance function representing the optical properties of the PMT and its light concentrator as well as any other aspect of the detector geometry such as shadowing. Also, the composition of the detector has to be considered at this point: For example, in some experiments a buffer region generating much less light is present. Concentrating these light distribution effects within the local detection efficiency $LD(\vec{x})$, we can rewrite Equation 13 as:

$$P(\vec{x}) = F(t(\vec{x})) \cdot LD(\vec{x}) \ . \tag{14}$$

At last this has to be normalised for each signal, leading to

$$P(\vec{x}) = \frac{F(t(\vec{x})) \cdot LD(\vec{x})}{\iiint F(t(\vec{x})) \cdot LD(\vec{x}) \cdot d\vec{x}} \ . \tag{15}$$

The resulting probability density distribution for a single signal is depicted in Fig. 3 showing the effect of the time distribution (left panel) and the additional influence of the light propagation effects (right panel).

To finally get a 3D topological picture of the event, the 3D probability density distributions of all signals belonging to the event have to be combined. Since we do not know which photons have been emitted from the same point, all signals have to be considered as being independent. Thus, the 3d probability density distributions of all signals have to be summed up:

$$P(\vec{x})_{total} = \sum_i P_i(\vec{x}) = \sum_i \left[\frac{F_i(t(\vec{x})) \cdot LD_i(\vec{x})}{\iiint F_i(t(\vec{x})) \cdot LD_i(\vec{x}) \cdot d\vec{x}} \right] \ . \tag{16}$$

Here, the index i indicates the individual signals. Thus the F_i have to be evaluated with the individual signal times $t_{signal,i}$ and the position P_i of the PMT which detected the signal, while LD_i is an attribute of this PMT depending on its position, optics and sensitivity.

The result is a 3d map of the expected mean number of detected photons $\langle N_{detected}(\vec{x}) \rangle$ coming from a given point. However, to get an impression of the energy deposition for a given event, not the number of detected photons from a given point is deciding but rather the number of photons emitted from that point $\langle N_{emitted}(\vec{x}) \rangle$. Therefore, every point of the 3d distribution has to be weighted by the inverse of the total signal detection efficiency $\eta(\vec{x})$ at that point:

$$\langle N_{emitted}(\vec{x}) \rangle = \frac{\langle N_{detected}(\vec{x}) \rangle}{\eta(\vec{x})} = \frac{P(\vec{x})_{total}}{\sum_{PMT} LD_{PMT}(\vec{x})} \tag{17}$$

In principle, the reconstruction is completed at this point. However, due to the large width of the time distribution of the individual signals, the picture may not seem

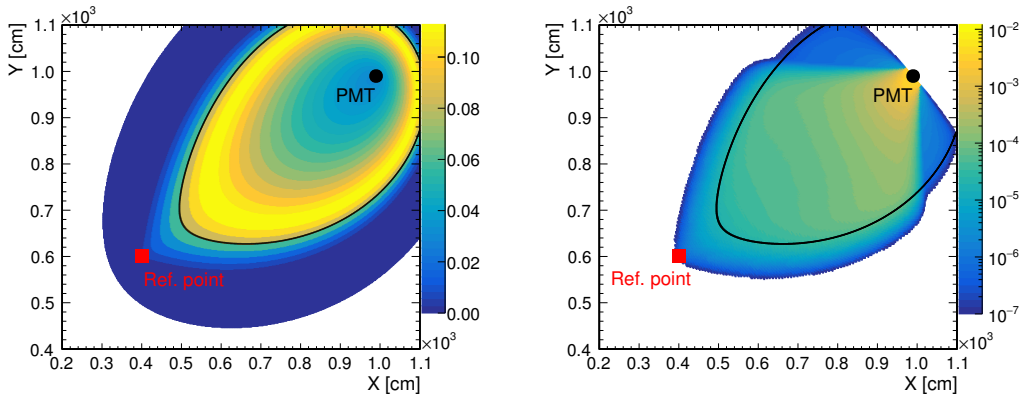

Figure 3: Unnormalized 2D versions of $\Phi_{j,k}(x)$ with (right) and without (left) the inclusion of the spatial probability $P_{\mathrm{det},j}(x)$ for the same configuration of photosensor and reference point as in fig:DropShapes. The photon hit time for the sharp isochrone (black line), calculated as in fig:DropShapes with the plus sign for the particle contribution, was set to 33ns.

very sharp. On the other hand, the large number of photons involved still generates a very good spatial resolution of the event topology. To extract this information, further algorithms are neccessary. For this purpose, standard algorithms developed originally for 2D image processing - like filtering, ridge-line finding, Sobel filter, etc. - can be adapted to accommodate 3D data.

Iteration procedure

So far, the individual 3D probability density distributions of all available signal photons have been added to get the total picture. This is the correct way - from the statistics point of view - if all signals are completely independent of each other. In contrast, if all signals are directly correlated, as is the case for a point-like event, the individual 3D probability distributions can be multiplied in order to get the most likely common point of origin in the most efficient way. For extended events, this is not possible, because not all of the signals belong to the same point. Then again, every point of the true event-topology is the origin of many detected photons and thus a correlation exist between these signals. In other words we have a mixure of correlated and uncorrelated information and need a way to exploit the correlation.

One way to take this into account is to divide the detector PMT-wise into equivalent subdetectors. If all of these subdetectors have enough signals to provide information about every point of the event topology, it is a robust approach to perform the above reconstruction for each of the subdetectors and then multiply the 3d topological distributions of all the subdetectors. In this way, the topological information gets much sharper. However, this also introduces a bias, as points which are already more prominent in the individual results of the subdetectors will be artificially enhanced.

To avoid this, another approach is followed here. The correlation we want to exploit is our knowledge that all signals belong to the same event and thus the same topology. If we dispose of a certain prior knowledge about that topology, we can

express this as a 3D probability density distribution $PM(\vec{x})$. Instead of calculating our topological 3D-picture from the completely independent 3D probability density distributions $P(\vec{x})_i$, we can now calculate this topology under the condition that it has to match our knowledge $P(\vec{x}|PM(\vec{x}))_i$. In other words, if we already have a 3d representation of the event, which we call in this context probability mask (PM), we can use this to reweight the 3D probability density distribution generated by every single photon prior to its normalisation: Thus Equation 15 becomes

$$P(\vec{x}|PM(\vec{x}))_i = \frac{F_i(t(\vec{x})) \cdot LD_i(\vec{x}) \cdot PM(\vec{x})}{\iiint F_i(t(\vec{x})) \cdot LD_i(\vec{x}) \cdot PM(\vec{x}) \cdot dV} \tag{18}$$

In principle, the choice of the probability mask is free, as long as it represents the prior knowledge of the event in an unbiased way. For example the results of the likelihood method in Section **??** could be used to predefine a volume where to look for energy depositions. The easiest way to generate a PM is then to give every point inside the volume of interest the value 1 and set the probability outside to zero. However, it turns out that sharp edges may negatively affect the reconstruction result: In this case, the normalisation enhances signals too much which only have a slight overlap with the PM. This often happens with signals from scattered photons, as they do not carry any topological information on the event and thus are only noise for the reconstruction. One way to cure this is to smoothen the edges of the selected region by adding a region where the PM slowly goes to zero, for instance a Gaussian flank.

A natural choice is to use the reconstruction as described in Section 1.2, i.e. without a PM, first. The result of this reconstruction then constitutes an unbiased representation of the event topology, which can then be used as the PM for a second iteration of the reconstruction. The result of this second reconstruction can again be fed back as a new PM into the reconstruction process. Thus an iterative procedure is created. The power of this iterative process can be seen in Fig. 4. Ultimately, this allows a close association of each signal photon with a certain volume of the event topology. This makes the energy deposition per unit length accessible as can bee seen in Fig. 4.

To improve the robustness and the convergence speed of the iteration procedure, we applied an additional artifice to produce the results presented in 4: If the full reconstruction result is used for the PM of the next iteration a small impreciseness enters the procedure. The reason for this is that the data used, was also used to generate the PM and the two are thus not completely independent from each other. This can lead to self-enhancement effects, if a certain region of the 3d probability density distribution under inspection is dominated by data from a single source (PMT). To avoid this, in principle every PMT would need its own PM, generated with the help of all the other PMTs. This however is impractical. A more convenient solution is to divide the dataset into two completely independent parts being as similar as possible, e.g. by just taking every second PMT for each part respectively. Then one of these datasets can be used to produce the PM for the other half of the PMTs and the other way round. By alternating between the two datasets in the iterative procedure self-enhancement can be suppressed. To use the full dataset for the final result, the last two iteration outputs must then be combined by adding them up.

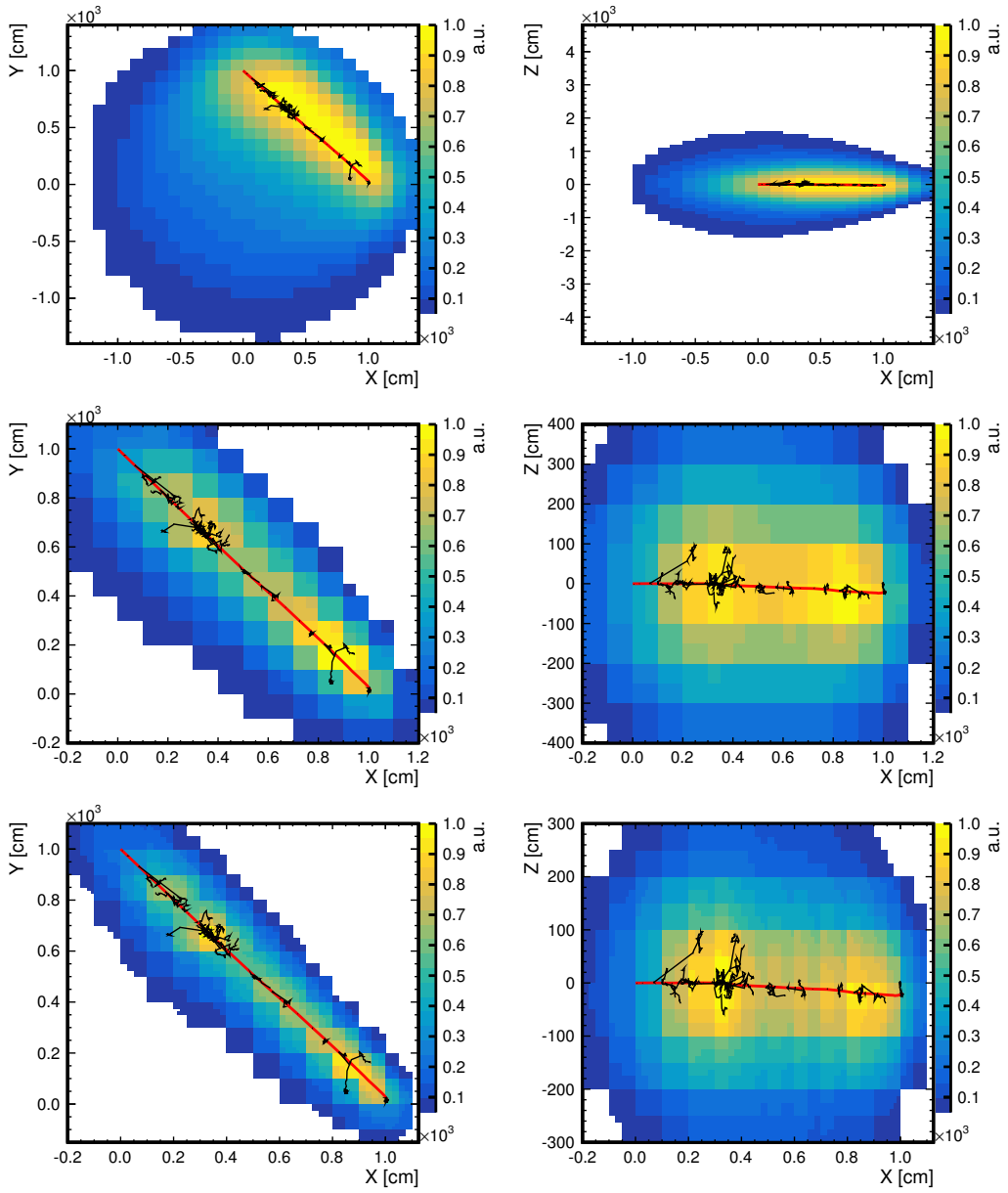

Figure 4: Reconstruction results after the iterations 0 (top), 8 (middle) and 21 (bottom) for a simulated muon with 3GeV initial kinetic energy in the cylindrical LENA detector projected along the symmetry axis (left) or a radial y-axis (right). The primary particle started at (0, 1000, 0)cm in the direction (1, −1, 0). Both the projected tracks of the primary particle (red) and of secondary particles (black) are shown. Note that both the axis scales and the sizes of the cells change due to the selection of a region of interest and the refinement of the reconstruction mesh. Moreover, the cell content is given in a.u. and rescaled such that the maximum content is 1. Some details on the actual reconstruction procedure are given in sec:Reconstruction.

Short summary

The whole procedure can be put into this logical sequence:

1. Get a reference point
2. Calculate drop-like surface for each signal
3. Smear the surface with the time profile of the signals
4. Add light distribution effects
5. Normalise the probability density distribution for each signal
6. Use the spatial-dependent light detection efficiency to go from detected light to emitted light
7. Use the result of emitted light as a probability mask and repeat everything starting from point 5

Since the probability mask will only start to affect everything during the normalisation of the single photon probability density distributions, the iteration can in principle begin at point 5 of this sequence. However, this is very memory intensive, since the raw results of each PMT have to be saved (the 3d representation of equation 14). Thus we choose to begin the iteration loop at point 2.

Results

So far this method has mainly been studied with the help of the LENA simulation. This simulation includes only an effective optical model and no Cherenkov light. Furthermore, it was assumed that every photon could be registered separatly. LENA has a coverage of 30% resulting in approximatly 250 detected photons per MeV. To reduce the computation time for the reconstruction an adaptive mesh was used. This allowed to establish a voxel size of 12.5 cm in the final iteration. More details about the simulation and the technical implementation of the topological reconstruction can be found in **??**.

To proof the robustness and show the potential of this method a large sample of fully contained muonswith energies between 1 and 10 GeV was used. An angular resolution between 1.4 at 1 GeV and 0.4 at 10 GeV could be achieved.

Application to Cherenov-light

Some modifications are needed for the application of this method to Cherenkov light. The most obvious one is the time profile $F(t)$ (equation 12), since the Cherenkov process emits the light instantaneously. Thus in most scenarios the timing profile of the photosensors will be the dominant factor, which can often be described by a Gaussian with the corresponding time resolution. However, chromatic dispersion of the Cherenkov light must be taken into account if sensors with very good time resolution (below 1 ns) are employed in detectors of the size of THEIA.

In addition the position dependent detection efficiencies also become direction dependent now, since the Cherenkov light is emitted only in a cone with respect to the particle direction. How to generate such direction dependent detection efficiencies is shown for example in []. However, in general they differ for different particles due to the different behaviour when passing through matter. Thus smaller or wider angular

distributions of the emitted Cherenkov light are generated. This is the same effect that allows to distinguish between electrons and muons based on the sharpness of the Cherenkov ring.

Since the idea of this method is to work without any hyphothesis, such a situation is unfortunate. To avoid this, we start instead with the basic method without any light distribution effect (detection efficiencies). Thanks to the good timing quality of the Cherenkov-light this already allows to define an accurate region of interest. Now, we calculate the angular distribution (with respect to the direction to the reference point) of all the signals for every point (voxel) in this region of interest. However, for each point we use only signals that match the point in time (the isochrone of the signal time representing equation 11 is close enough to the point). This angular distribution can then be used to calculate the local detection efficiency for each PMT at this position in the detector. Once we have this we can proceed with the same iteration process used for the scintillation light.

Separation of Cherenkov and scintillation light

1.3 Low energies reconstruction

by Andrey